SI Materials and Methods

Mice, keratinocytes, IHC and IF: Mice used in this study were: *Rb* and *Rb;E2f* chimeras (Parisi et al. 2007; Parisi et al. 2009); Rbc/c (Sage et al. 2003); K14Cre (Dassule et al. 2000); and K14CreERT (Vasioukhin et al. 1999). Tissues were treated and stained as described previously (Parisi et al. 2007), or OCT-embedded for histology and IHC. Primary keratinocytes were isolated from E18.5 embryos and cultured as described previously (Hodivala-Dilke et al. 1998) in 0.05 mM CaCl₂ on Col1 coated surfaces. AdGFP and AdCreGFP infections were conducted at 10 MOI for 3 hrs. Junctions were induced with 1.8mM Ca2+. Rock inhibitors (Calbiochem) were added at $10\mu M$ Y27632 and 5 μM H-1152, and BrdU at 33 μM . For IF, 10 μm cryosections or coverslips fixed with 4% PFA for 15' were incubated o/n at 4°C with primary antibodies and detected with Alexa Fluor-conjugated secondary antibodies (Invitrogen), plus Alexa Fluor-conjugated phalloidin and dapi, to also visualize Factin and nuclei. DeltaVision microscope images were deconvolved using SoftWoRx acquisition software (Applied Precision) and quantified by ImageJ. P values were calculated with Student's t-test.

Migration and wound healing assays: For Boyden chambers, 10^5 cells were plated in triplicate on 8μm pore, 24 well transwell plates. Migrated cells were detected by crystal violet after removing cells from the top chamber by Q-tip. For *in vitro* scratch assays, confluent cell layers were incubated with 1.8mM Ca for >24 hrs and scratched with yellow tips. Two wounded areas/plate/embryo were photographed over time and the gaps quantified by ImageJ. For time lapse microscopy, $5x10^4$ cells

were plated on 12 well glass bottom plates (MatTek), photographed every 10 min for 15 hours and the GFP+ cells analyzed by Imaris imaging software. P values were calculated with Student's t-test. For *in vivo* wound healing, 2 months littermates were painted with tamoxifen (2.5 mg in EtOH) for 11 days, and a skin-thick 1 cm incision monitored daily for 5 days. Genomic DNA was extracted and analyzed by PCR.

Protein and RNA: For protein, cells were lysed in NP40 buffer+ protease and phosphatases inhibitors, or 1% SDS 60mM Tris-Cl pH 6.8 at 95°C, and processed as described (Parisi et al. 2007). For mRNA, total RNA was extracted using RNeasy Mini+RNAse-Free DNAse Set kits (Quiagen). cDNA was generated using Superscript III (Invitrogen) and 10ng/sample (≥3 cell lines) assayed in duplicate by qPCR on a 7500 real time PCR system (Applied Biosystem) using SybrGreen. Results were normalized to ubiquitin, and P values were calculated with Student's t-test.

Primary antibodies: krt 6 sc-22481; krt 14 Neomarkes LL002; krt 10 Covance PRB-159; Ki67 BD 550609; E-cad BD610181 or CS 3195; Paxillin BD 610620; Vinculin Sigma V9131; P-MLC2(Ser19) CS 3675; MLC2 CS 3672; aPKCζ sc-216; ZO1 Invitrogen 617300; Par3 Upstate (Millipore) 07-330; RhoA CS 2117; pRB Pharmigen 554136; β-tubulin Sigma T7816; α-tubulin AB15246; Par6 Sigma 9547; and BrdU BD 3475800.

Primers: All 5' to 3'. mypt1: F-gttccagtgaggaggaggaggag, R-aagccatgggctttgtctta; par-6:
F-gggttccaggtatcttcatc, R-gacctcaaggatctcatcac; prickle-: F-cagagaagctccacatcag R-ggcaagcatgcgaaatag; frizzled-2: F-cacggtcaccacctattt, R-tgcagccttctttcttagt; mlc2: F-

gtgttcgccatgtttgac, R-ggcatcagtgggattctt; *par-3*: F-aacaactgtcccaacgcgagaa, R: tttggttgaggcgtgagcacta; *Z01:* F-aaatgagaagcagacgcccact, R-accagtttcatgctgggcctaa; *aPKCÇ*: F-acggacaaccctgacatgaaca, R-tgctgcggaagaaagcatgaga; *cdc42:* F-tgttggtgatggtgctgttggt, R-agtccaagagtgtatggctctcca; *rac1*: F-tgcctgctcatcagttacacga, R-ttcttgtccagctgtgtcccat; *E-cadherin*: F-cagccttcttttcggaagact, R-ggtagacagctccctatgact; *rock1:* F-gctgaatgacatgcaagcgcaa, R-tttgcccgcaactgctcaat; *rhoA:* F-tgttggtgatggagcttgtggt, R-tcaaacaccgtgggcacataga; *p107:* F-tctgacaatggccacaaccaca, R-ttggcgataccatgcaaaggga; *cyclin E1:* F-tgtttttgcaagacccagatga, R-ggctgactgctatcctcgct.

References (not included in text).

- Dassule, H.R., Lewis, P., Bei, M., Maas, R., and McMahon, A.P. 2000. Sonic hedgehog regulates growth and morphogenesis of the tooth. *Development* **127**(22): 4775-4785.
- Hodivala-Dilke, K.M., DiPersio, C.M., Kreidberg, J.A., and Hynes, R.O. 1998. Novel roles for alpha3beta1 integrin as a regulator of cytoskeletal assembly and as a trans-dominant inhibitor of integrin receptor function in mouse keratinocytes. *J Cell Biol* **142**(5): 1357-1369.
- Parisi, T., Bronson, R.T., and Lees, J.A. 2009. Inhibition of pituitary tumors in Rb mutant chimeras through E2f4 loss reveals a key suppressive role for the

- pRB/E2F pathway in urothelium and ganglionic carcinogenesis. *Oncogene* **28**(4): 500-508.
- Sage, J., Miller, A.L., Perez-Mancera, P.A., Wysocki, J.M., and Jacks, T. 2003. Acute mutation of retinoblastoma gene function is sufficient for cell cycle re-entry.

 Nature 424(6945): 223-228.
- Vasioukhin, V., Degenstein, L., Wise, B., and Fuchs, E. 1999. The magical touch: genome targeting in epidermal stem cells induced by tamoxifen application to mouse skin. *Proc Natl Acad Sci U S A* **96**(15): 8551-8556.

Supplemental Figure Legends

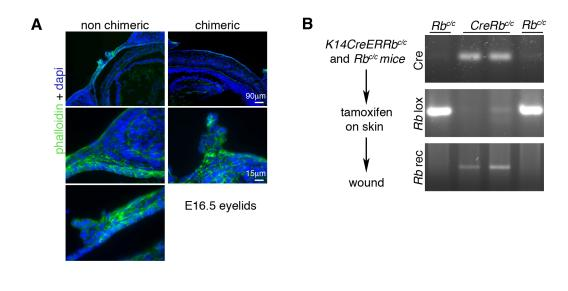
Supplemental Figure 1. (A) Phalloidin staining of E16.5 *Rb*-/- chimeric eyelids shows that the *Rb*-/- eyelid tips fail to attach, extend and stretch over the cornea, and present with few and disorganized F-actin cables (phalloidin green, nuclei stained with dapi in blue). (B) *Left*, experimental scheme of the *in vivo* wound healing assay. *Right*, PCR analysis of *K14CreRb*-/-c and *Rb*-/-c epidermis topically treated with tamoxifen confirms efficient recombination of the *Rb* locus in *K14CreRb*-/-c mice. (C) LacZ staining of E18.5 *Rb*-/-;*E2f3*-/- and *Rb*-/-;*E2f4*-/- chimeric embryos shows that the EOP is not rescued by concomitant loss of these *E2fs* indicating that the *Rb* mutant phenotype does not depend on these E2Fs.

Supplemental Figure 2. Keratinocytes were isolated from the skin of E18.5 $Rb^{c/c}$ embryos and infected with AdCreGFP to ablate Rb or with AdGFP as a paired wildtype control. Western blot analysis of cell extracts isolated 48 hours post-infection shows loss of pRB protein in the Cre-infected samples.

Supplemental Figure 3. (A) Phase contrast images show that *Rb* mutant keratinocytes are much rounder than wild type. (B) PP1, a phosphatase for MLC2, is inactivated by Rock through phosphorylation on the Thr853 residue of MYPT1, its regulatory subunit. Western blot analyses show that *Rb* loss caused increased phosphorylation of the Thr853 residue on MYPT1. Thus, PMLC2 accumulation in *Rb* deficient cells, results from direct MLC2 phosphorylation, and phosphatase inactivation, which are both caused by activation of the RhoA-Rock pathway. (C) qRT-PCR analyses show no difference in mRNA of the main RhoGTPases or their

targets in wildtype and $Rb^{-/-}$ keratinocytes cultured in low Ca medium. Note that both p107 and cyclin E levels are unchanged upon acute ablation of Rb in line with comparable cell proliferation rate in low Ca conditions.

Supplemental Figure 4. (A) Upon addition of CaCl2 for 3 hrs, *Rb* mutant cells proliferate at a similar rate than wildtype as measured by BrdU incorporation. (B) qPCR analyses of mRNA levels of PAR, PCP, and junctional components show no significant differences between Rb-/- and wildtype cells exposed to high Ca for 24 hrs. Conversely, the E2F targets, cyclin E and p107, are upregulated upon Rb loss in line with the ectopic proliferation occurring in these conditions. Western blot analyses of cell treated with calcium for 0, 3, or 24 hours confirms that junctional and PAR proteins are expressed at similar levels in *Rb* deficient and wildtype keratinocytes. (C) Adherens and tight junctions do form in Rb-/- cells after 24 hrs Ca, but they appear to be less apical and defined than in wildtype controls. (D) Although treatment with the Rock inhibitor H1152 disrupts the actin cytoskeleton and junctions in wildtype and $Rb^{-/-}$ cells exposed to Ca for 3hrs, aPKC still accumulates at the plasma membrane in the $Rb^{-/-}$ cells suggesting that its upregulation may be independent of RhoA in this context. Note that this coincides with similar levels of P-MLC2 proteins in the confluent monolayers.





E18.5 chimeras

